IRAQI Academic Scientific Journals

University of Kirkuk Journal For Administrative and Economic Science (2024) 14 (3): 132-140

UKJAES

University of Kirkuk Journal For Administrative and Economic Science

ISSN 2222-2995
University of Kirkuk Journal For Administrative and Economic Science

Hamood Ahmed Jabbar. A Color Image Enhancement Using Statistical Techniques. *University of Kirkuk Journal For Administrative and Economic Science* (2024) 14 (3):132-140.

A Color Image Enhancement Using Statistical Techniques

Ahmed Jabbar Hamood [1]

[1] *Universty of Sumer, College of Adminstration and Economics, Department of Statistics, Dhi Qar, Iraq*

ahmed.jabbar.h89@gmail.com[1]

Abstract: Noise, particularly Gaussian noise, can distort images and reduce information. The James Webb Space Telescope (JWST) is vital for understanding the universe and capturing images that inspire people. This paper introduces several nonlinear filters to remove Gaussian noise from the Jupiter Image. The filters consider similarities and distances between central pixels and preserve edges as advanced features. These filters are crucial for advancing scientific knowledge, showcasing technological prowess, and contributing to the broader mission of exploring the cosmos. The results show that the Bilateral filter provides high performance in restoring images under different Gaussian noise densities compared to the non-local mean (NLM) denoising filter, returning high values for peak signal to the noise ratio (PSNR) and structural similarity index measure (SSIM) respectively in the case of 50, 75 per cent of noise ratio, which exceeds what the filters produced as in another noise ratio.

Keywords: Image Denoising; Image Restoration; Gaussian Noise; Non-Local Means Filter; Bilateral Filter.

تحسين الصور الملونة باستخدام التقنيات الاحصائية

م.م. احمد جبار محمود[1]

[1] *جامعة سومر-كلية الادارة والاقتصاد، قسم الإحصاء، ذي قار، العراق*

المستخلص: الضوضاء، وخاصة الضوضاء الغوسية، يمكن أن تؤدي تشويه الصور وتقليل المعلومات، ويعد تلسكوب جيمس ويب الفضائي (JWST) أداة او واسطة حيوية لفهم الكون والتقاط الصور التي تلهم الناس، في هذا البحث استخدمنا لعديد من الفلاتر او المرشحات غير الخطية لإزالة الضوضاء الغوسية من صورة المشتري، اذ تأخذ هذه المرشحات في الاعتبار أوجه التشابه والمسافات بين العناصر الصورية الاساية وتحافظ على الحواف كميزات متقدمة في الوقت نفسه، وتعتبر هذه المرشحات ضرورية لتطوير المعرفة العلمية، وعرض البراعة التكنولوجية، والمساهمة في المهمة الأوسع لاستكشاف الكون، وأظهرت النتائج أن المرشح الثنائي يوفر أداءً عاليًا في استعادة الصور تحت كثافات ضوضاء غوسية مختلفة مقارنةً بمرشح تقليل الضوضاء للمتوسط غير المحلي (NLM)، مسجلا قيم جودة صورية عالية باستخدام معيار اشارة الذروة إلى نسبة الضوضاء (PSNR) وقياس مؤشر التشابه الهيكلي (SSIM) على التوالي في حالة ٥٠، ٧٥ بالمائة من نسبة الضوضاء.

الكلمات المفتاحية: تخفيض الضوضاء الصوري، تحسين الصور، ضوضاء غاوسية، مرشح المتوسط غير المحلي، المرشح الثنائي.

Corresponding Author: E-mail: ahmed.jabbar.h89@gmail.com

INTRODUCTION

Satellite images are essential in many real-world applications because they offer an accurate and clear vision of the issue being investigated [1]. These applications include monitoring the velocity of planets, galaxies, and other astronomical objects the rate of climate change and the rise and fall of ocean levels. A digital computer can manage and store the satellite image, represented as a sequence of integers [15]. An image is split into tiny fragments called pixels to convert into numbers [26]. Satellite images are affected by transmission and acquisition noise, just as other image types [23]. This may impact studies and image analysis. The noise must be reduced or eliminated to evaluate and examine the image(s). Noise in satellite images is an unwanted physical phenomenon resulting from atmospheric layer fluctuations [30]. Mention that there are various types of noise, with Gaussian noise being the most prevalent [17]. Each pixel in the noisy image [24] is the sum of the genuine pixel value and a random noise value distributed using the Gaussian distribution. This statistical noise has a probability density function that resembles a normal distribution and is known as additive white Gaussian noise (**AWGN**) [3].

This paper discusses the formation of noise on telescope images throughout the acquisition or transmission phase. Image quality is diminished by this phenomenon, which also lowers the quality of the analysis and interpretation. This paper aims to reduce this noise by applying nonlinear algorithms to preserve as much information as possible about space telescope images since space telescope images are crucial for scientific research and study. Nonlocal mean (**NLM**) and Bilateral (**BF**) are some of the best filters for image DE noising and edge preservation. **NLM** DE noising algorithms, locate adjacent pixels in a broad search window and determine each pixel's weight by summing up and comparing its similarities and intensities [7]. Buades created these algorithms [21]. On the other hand, Manduchi's [31] simple, stable, and no iterative **BF** minimizes noise and stays away from edges while taking into consideration variations in both spatial and intensity from the central pixel [6]. Moreover, we suggest an powerful image enhancement method that takes under consideration the outcomes of greater noise on person pixels within the photo. It is necessary to choose the best smoothing parameter for each photograph pixel. So, our proposed filter out seeks to extract a smoothing parameter as a first step, then use it to estimate the Gaussian density feature of the photograph, and eventually follow a de-noising approach to the calculated Gaussian feature.

In recent years, many researchers have tried to reduce noise in their experiments using these filters, this study highlights the most notable results on image degradation. Thus, we are able to use these methods for the desired learning purpose and improve their effectiveness by using the materials and enhancements provided. For example, Hossain and Habib [8] found that using multiple reconstruction NLM filtering (MRNLM) to remove irrelevant information from auxiliary images MRNLM method increased SNR characteristic measurements from 25.1 to 28.8 when using Gaussian filtering is being used The effectiveness of NLM using noise algorithm in MR imaging To test it, Heo et al [18] conducted a detailed study, which provided evidence of an accurate method for diagnosis and their results shows that the NLM breakdown process is a viable method. Feng and Pan, [14] proposed improved methods based on diverse functions and quick or optimization terms are intended to yield more insightful findings. A new three-step approach for enhancing infrared images based on the relativity of the Gaussian adaptive bilateral filter. By multiplying the image by the suggested weight coefficient, dividing it by the relativity of the Gaussian-adaptive bilateral filter, and combining the processed base layer and detail layer, the suggested approach successfully boosts the contrast of infrared images. Chen and Gao, [12] proposed an NLM algorithm based on the fractional compact finite difference scheme (FCFDS) to reduce speckle noise in OCT images. When compared to integer order difference operators, FCFDS uses more local pixel data. Simulations demonstrate that, in comparison to other cutting-edge de-speckling techniques, the suggested method significantly reduces noise and preserves image details. Wagner et al., [32] proposed a hybrid denoising technique that combines a convolutional deep learning denoising network with a set of trainable joint bilateral filters (JBFs) to predict the guidance image. The outcome demonstrates a high level of noise reduction efficacy. Nabahat et al., [28] proposed a bidirectional whale optimization algorithm (WOA) filter for image denoising depending on the selection of appropriate parameters. Appropriate parameter selection is necessary for the bilateral filter to work properly. Using the weighted sum of PSNR and SSIM as a fitness function during filter design, the WOA method improves the filter's parameters. The outcomes demonstrate that the suggested strategy outperforms the others. Fabian et al., [33] suggested a bilateral filter that can be incorporated into any deep learning algorithm and optimized only through data-driven methods by calculating the gradient flow toward its input and hyperparameters. The proposed method can compete with state-of-the-art denoising architectures. Huihua et al., [20] combined an improved NLM de noising technique with the Laplacian of the Gaussian operator to more precisely extract gradient information from images. The proposed approach preserves the image edge while suppressing noise to recover high PSNR CT images.

1. Noise

Noise is unwanted or random variations in pixel values that can distort the true representation of the scene or information being captured [2]. It can be considered as an undesirable interference that obscures or degrades the quality of the image. Noise manifests as random fluctuations in pixel values and is typically unpredictable, this randomness is due to various factors in the imaging process [25]. Gaussian noise, also known as additive white gaussian noise (**AWGN**) [27]. It is one of the most common types of noise. It is a random noise that follows a Gaussian (normal) distribution. It appears as a subtle, smooth variation in pixel values across the image [29].

2. NON-LOCAL MEAN FILTER (NLM)

A. Buades et al. (2010) initially presented the Non-Local Mean Filter (NLM) technique, which is predicated on a non-local average of all pixels [13]. this nonlinear filter is used to eliminate Gaussian noise from photographs while maintaining image details [5]. The estimated value NL[v](i) for a pixel (i) in the noise image $v = v\{v(i) \mid i \in I\}$ is computed as.

$$NL[v] = \sum_{j \epsilon I} w(i,j) v(j) \qquad (1)$$

The weights, represented by w (i, j), are established based on how similar pixels (i) and (j) are to each other. They also need to satisfy the conventional requirements $\sum_j w(i, j) = 1$ and $0 \leq w(i, j) < 1$. [10]. The two pixels (i) and (j) are similar when the vectors v(Ni) and v(Nj) have identical intensities. A fixed-size square neighbourhood with a pixel (k) at its center is indicated by (NK). A diminishing function of the weighted Euclidean distance is used to quantify the similarity.

$$\left\| v(N_i) - v(N_j) \right\|_2^2 \qquad (2)$$

In noisy neighbourhoods, the Euclidean distance increases the following equality [35].

$$\left\| V(N_i) - v(N_j) \right\|_2^2 = \left\| v(N_i) - v(N_j) \right\|_2^2 + 2\sigma^2 \qquad (3)$$

It explains the resilience of the (NLM) since the Euclidean distance is predicted to preserve the order of similarity between pixels [36]. The weights are defined as follows:

$$w(i,j) = \frac{1}{Z(i)} e^{\frac{-\left\| v(N_i) - v(N_j) \right\|_2^2}{h^2}} \qquad (4)$$

Z(i) is the normalising constant and (h) is the filtering degree or smoothing parameter.

$$Z(i) = \sum e^{\frac{-\left\|v(N_i)-v(N_j)\right\|_2^2}{h^2}} \quad (5)$$

It regulates the weights' decay as a function of Euclidean distances by controlling the exponential function's decay.

3. BILATERAL FILTER (BF)

It is a nonlinear filter used to smooth images and maintain their edges [4]. Unlike conventional convolutional filters, it measures proximity in intensity space using a different kernel [16]. A weighted average of nearby pixels is represented by the symbol [1].

$$BF[I]_p = \frac{1}{W_p}\sum_{q\in s} G_{\sigma_s}(\|p-q\|)G_{\sigma_r}(\|I_p - I_q\|)I_q \quad (6)$$

where $\{G_{\sigma_s}\}$ and $\{G_{\sigma_r}\}$ is the spatial filtering and Gaussian range respectively, (Wp) is the normalization factor, which is defined as follows [22]:

$$W_p = \sum_{q\in s} G_{\sigma_s}(\|p-q\|)G_{\sigma_r}(\|I_p - I_q\|)I_q \quad (7)$$

The amount of filtering that is done to image (I) will depend on the values of σ_s and σ_r. The influence of (q) pixels is lessened by the Gaussian range G_{σ_s} when their intensity values deviate from (Ip). A Gaussian weight called G_{σ_s} is used to reduce the impact of far-off pixels.

4. DISCUSSION OF RESULTS

The experiment was conducted by adding **AWGN** with **zero** mean and **0.01** variance to the approved image as shown in **Figure 1**, which is the **JWST** image of Jupiter(https://webb.nasa.gov/). **JWST** is expected to be the most influential observatory in the next ten years, with thousands of astronomers utilizing it globally. It looks at every phase of the history of our universe, from the earliest bright lights seen after the Big Bang theory to the formation of solar systems that might support life on planets like Earth and the evolution of our own Solar System. Thus, this image needs to be pure and unclouded. Taking these image significances into consideration. So, the process of eliminating noise is fundamental and significant in this instance . We applied the chosen filters—whose MATLAB code was written—after adding varying percentages of Gaussian noise to the selected image to assess the effectiveness of the filters.

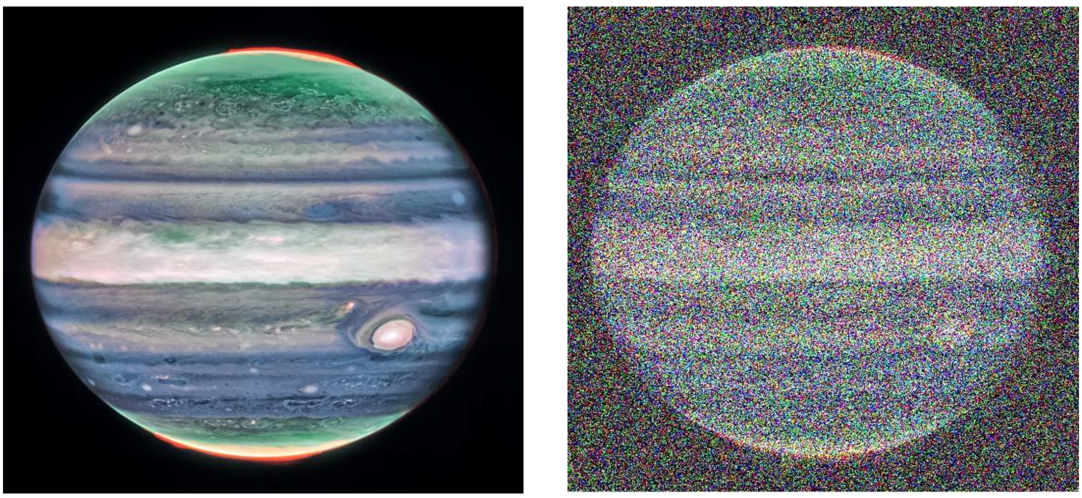

A B

Figure (1): (A) Jupiter Original Image, (**B**) Jupiter Gaussian Noise Image.

The Structural Similarity Index Measure (**SSIM**) and the Peak Signal Noise Ratio (**PSNR**) are used to calculate the quality of the results that are obtained. **PSNR** is a quality metric that is widely used to assess the quality of reconstruction for images and videos [19].

$$\mathrm{PSNR} = 10 * \log_{10} * \left(\frac{255^2}{\mathrm{MSE}_{(x,y)}}\right) \qquad (8)$$

Where:

$$\mathrm{MSE}_{(x,y)} = \frac{1}{MN}\sum_{i=1}^{M}\sum_{j=1}^{n}(x_{ij} - y_{ij})^2 \qquad (9)$$

Where $\{x_{ij}\}$ the clean image, $\{y_{ij}\}$ the noisy image. However, **SSIM** is a quality metric that assesses the degree of similarity between the two digital image structures [34]. It is given by the following equation:

$$\mathrm{SSIM} = (l(x,y))^{\alpha} * \left(c(x,y)\right)^{\beta} * (s(x,y))^{\gamma} \qquad (10)$$

Which represent three weights with the exponents (α), (β), and (γ), respectively [9].

$$I(x,y) = \frac{2\mu_x\mu_y + C_1}{\mu_x^2 + \mu_y^2 + C_1} \qquad (11)$$

$$C(x,y) = \frac{2\sigma_x\sigma_y + C_2}{\sigma_x^2 + \sigma_y^2 + C_2} \qquad (12)$$

$$S(x,y) = \frac{\sigma_{xy} + C_3}{\sigma_x\sigma_y + C_3} \qquad (13)$$

where the small quantities for numerical stability are C1, C2, and C3.
the results showed that the NLM filter outperforms Bilateral filters in terms of noise removal, recording a (**34.47 PSNR**), and (**0.92 SSIM**) respectively as shown in **Table 1**. Where the Bilateral filter ranks second with **31.62 PSNR** and **0.82 SSIM**. **Figure 2** displays the images that have been restored.

Table 1: PSNR and SSIM Values for The Restored Images at Each Filter

Filters	**Image Quality Measurements**	
	PSNR	**SSIM**
NLM	34.47	0.92
Bilateral	31.62	0.82

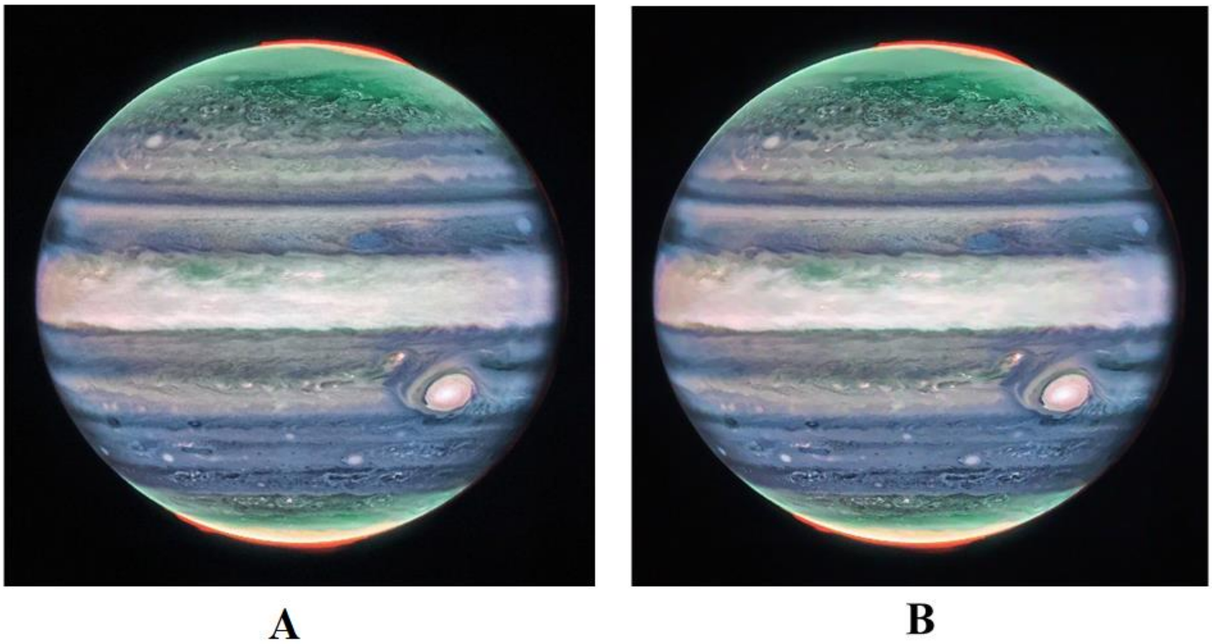

FIGURE (2). Restored Image at 0.01 Noise Ratio by (**A**) NLM Filter, (**B**) Bilateral Filter

Instead of focusing only on the immediate neighborhood, the NLM averages pixel values based on the similarity of patches throughout the entire image. A patch that is centerd on each pixel in the image is defined. A similarity metric is used to determine how similar the patch surrounding the current pixel is to the patches surrounding every other pixel in the image. Utilizing these acquired similarity values, weights for every pixel are determined. The similarity between the patch surrounding the current pixel and patches surrounding other pixels is represented by these weights. A weighted average of the pixel values in the patches surrounding each pixel—weights chosen based on how similar they are to the patch surrounding the current pixel—is used to compute the denoised value for that pixel. Taking lines from the whole image rather than just the surrounding areas. In contrast, the two-dimensional filter uses a demising method that takes into account both the near-field and intensity similarities of individual pixels Each pixel has a filter-defined window of bars that specifies the area separating the central pixel from pixels a in the surrounding area. Additionally, it calculates the pixel-to-pixel intensity difference (also known as similarity) between the center pixel and its neighbors. Each neighboring pixel's weight is determined by the Bilateral Filter based on its spatial proximity as well as its intensity similarity. The filtering process assigns higher weights to pixels that are close to each other spatially and have similar intensities. Next, using the spatial and intensity factors as weights, the filter computes a weighted average of the pixel values inside the window.

when the noise ratio increased, the bilateral filter superiority over the NLM filter in terms of noise removal persisted as the result shown in **Table 2**. In 50% and 75% noise densities, the bilateral filter has noise density values of 32.02 PSNR, 0.98 SSIM at 50%, 32.56 PSNR, and 0.99 SSIM at 75%. Thus, we observe that the bilateral filter forward to first place when the noise ratio increased, having previously placed second when the noise level was 0.01. As if the bilateral filter reduces noise while maintaining image edges because it gives pixels that are both spatially close and have similar intensity values more weight. This gives the filtered image a smoother visual quality by maintaining edges and reducing noise without sacrificing important features. On the other hand, the nonlocal mean filter is a versatile and effective denoising technique that considers the overall structure of an image. However, because it is computationally demanding, it needs to be adjusted and modified to make it more practical for use in real-world applications.

Table 2: PSNR and SSIM Values of The Restored Images Calculated at Different Noise Ratio

Filters	Image Quality Measurements			
	50% of Noise Ratio		75% of Noise Ratio	
	PSNR	SSIM	PSNR	SSIM
Bilateral	32.02	0.98	32.56	0.99
NLM	19.28	0.82	18.21	0.82

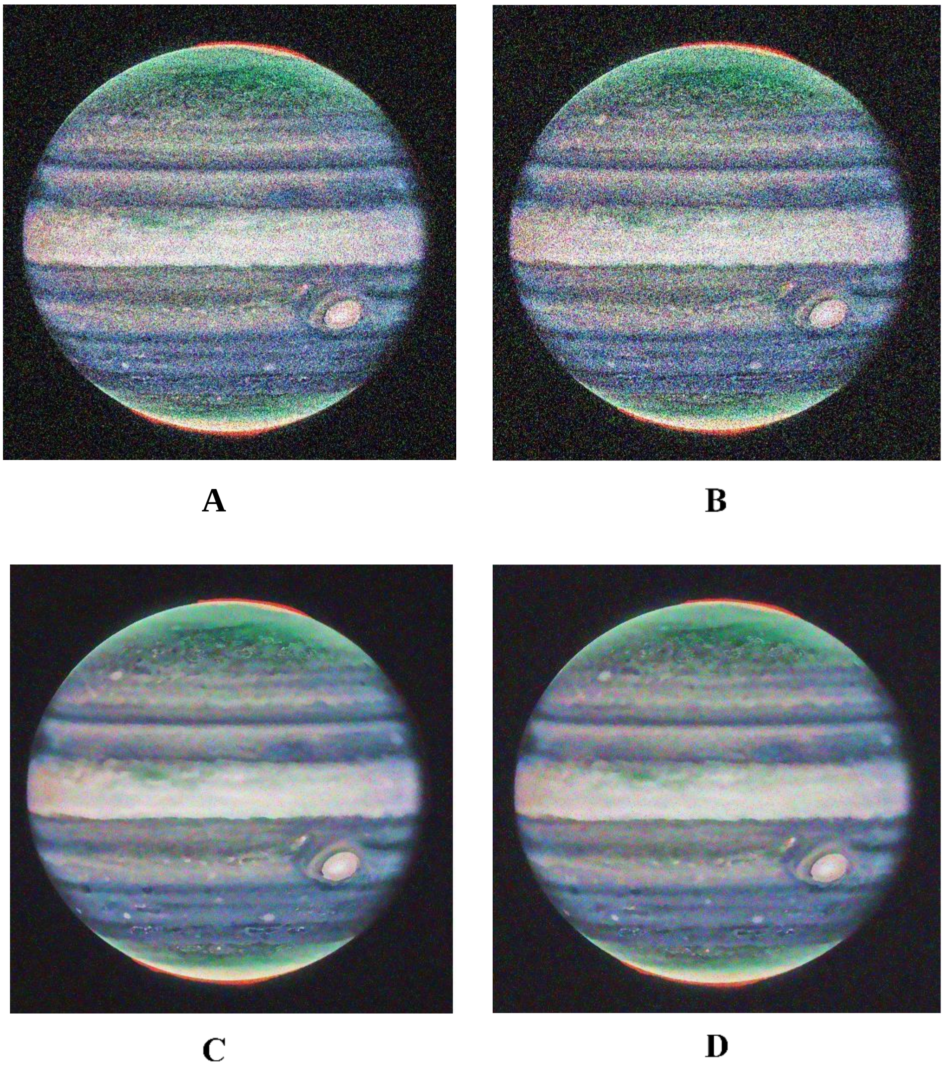

FIGURE (3). Restored Image by (**A**) Bilateral Filter at 0.5 noise ratio, (**B**) Bilateral Filter at 0.75 noise ratio (**C**) NLM Filter at 0.5 noise ratio, (**D**) NLM Filter at 0.75 noise ratio.

5. Conclusion

The bilateral filter provides a comprehensive image denoising method that separates noise and image structure, it reduces noise while preserving image features like edges and textures. The bilateral filter is adaptable, allowing easy parameter adjustments for different noise levels, and also provides quantitative metrics for evaluation, allowing objective comparison of different denoising methods and parameter settings. So, the outcomes demonstrate how adaptable the bilateral filter was in lowering noise levels without sacrificing any of the original image's characteristics. It moved the PSNR more than 20 degrees away from its nearest filter and achieved a high image quality index. On the other hand, the NLM filter assigns more weight to pixels that are both spatially close and have similar intensity values, it effectively reduces noise while maintaining image edges. In this manner, critical features are retained while noise is reduced and edges are maintained, giving the filtered image a smoother visual quality. To effectively remove noise while maintaining edges and image structures, the NLM filter takes into account patches from the entire image instead of just the immediate neighbourhood. This method is based on the logical assumption that similar image patches will probably contain similar image structures and should, thus, effectively aid in denoising. The ability of NLM to handle a variety of noise types, such as additive Gaussian noise, is one of its main advantages. However, NLM can be computationally demanding, particularly for large images or when comparing a large number of patches.

ACKNOWLEDGEMENT

The image of Jupiter is one of the images from the James Webb space telescope (JWST) that the author is grateful for being provided by the US National Aeronautics and Space Administration Agency (NASA) https://webb.nasa.gov/.

REFERENCES

1. Abdul Wadood, M. and Ghalib, A. (2018). Use Some Statistical Algorithms in Mock Hacking Satellite Images. *Journal Of Economics and Administrative Sciences*, Vol. 108, No. 24, pp.474–487.
2. Abdul Wadood, M. and Ghalib, A. (2019). Split and Merge Regions of Satellite Images Using the Non-Hierarchical Algorithm of Cluster Analysis. *Journal Of Economics and Administrative Sciences*, Vol. 25, No. 111, pp.466–484. https://doi.org/https://doi.org/10.33095/jeas.v25i111.1638.
3. Ali, M. (2018). MRI Medical Image Denoising by Fundamental Filters. *High-Resolution Neuroimaging - Basic Physical Principles and Clinical Applications*, Vol. 43, No. 17, pp.658–666. https://doi.org/10.5772/intechopen.72427.
4. Anchal, A., Sumit, B., Bhawna, G., Ayush, D. and Sunil, A. (2018). An Efficient Image Denoising Scheme for Higher Noise Levels Using Spatial Domain Filters. *Biomedical and Pharmacology Journal*, Vol. 11, No. 2, pp.625–634. https://doi.org/10.13005/bpj/1415.
5. Angella, S., Ari, S. and Rini, I. (2019). Application of Denoising Non-Local Mean Filter (NLM) in MRI Brain Image T2WI TSE SENSE. *International Journal of Allied Medical Sciences and Clinical Research (IJAMSCR)*, Vol. 7, No. 3, pp.1033–1039.
6. Angulo, J. (2013). Morphological Bilateral Filtering. *SIAM Journal on Imaging Sciences*, Vol. 6, No. 3, pp.1790–1822. https://doi:10.1137/110844258.
7. Anh, N. (2014). Image Denoising by Adaptive Non-Local Bilateral Filter. *International Journal of Computer Applications*, Vol. 99, No. 12.
8. Arabi, H, and Habib Z. (2020). Non-Local Mean Denoising Using Multiple Pet Reconstructions. *Annals of Nuclear Medicine*, Vol. 35, No. 2, pp.176–186. https://doi.org/10.1007/s12149-020-01550-y.
9. Bakurov, I., Marco, B., Raimondo, S., Mauro, C. and Leonardo, V. (2022). Structural Similarity Index (SSIM) Revisited: A Data-Driven Approach. *Expert Systems with Applications*, No. 189. https://doi.org/10.1016/j.eswa.2021.116087.
10. Buades, A., B. Coll, and Morel, M. (2005). A Non-Local Algorithm for Image Denoising. *IEEE Computer Society Conference on Computer Vision and Pattern Recognition (CVPR'05)*, No. 16. https://doi.org/10.1109/cvpr.2005.38.
11. Chen, B., Yi-Syuan, T. and Jia-Li, Y. (2020). "Gaussian-Adaptive Bilateral Filter." *IEEE Signal Processing Letters*, No. 27, pp.1670–1674. https://doi.org/10.1109/lsp.2020.3024990.
12. Chen, H. and Jing, G. (2022). Non-Local Mean Denoising Algorithm Based on Fractional Compact Finite Difference Scheme Effectively Reduces Speckle Noise in Optical Coherence Tomography Images. *Micromachines*, Vol. 13, No. 12, pp.2039-2039. https://doi.org/10.3390/mi13122039.
13. Dore, V. and Cheriet, M. (2009). Robust NL-Means Filter with Optimal Pixel-Wise Smoothing Parameter for Statistical Image Denoising. *IEEE Transactions on Signal Processing*, Vol. 57, No. 5, pp.1703–1716. https://doi:10.1109/tsp.2008.2011832.
14. Feng, X. and Zhongliang, P. (2021). Detail Enhancement for Infrared Images Based on Relativity of Gaussian-Adaptive Bilateral Filter. *OSA Continuum*, Vol. 4, No. 10, pp.2671-2676. https://doi.org/10.1364/osac.434858.
15. Ghalib, A. and Abdul Wadood, M. (2020). Using Multidimensional Scaling Technique in Image Dimension Reduction for Satellite Image. *Periodicals of Engineering and Natural Sciences*, Vol. 8, No. 1, pp.447–454. http://dx.doi.org/10.21533/pen.v8i1.1171.

16. Ghosh, S., Pravin, N. and Kunal, C. (2018). Optimized Fourier Bilateral Filtering. *IEEE Signal Processing Letters*, Vol. 25, No. 10, pp.1555–1559. https://doi.org/10.1109/lsp.2018.2866949.
17. Hambal, A., Zhijun, P. and Faustini, I. (2017). Image Noise Reduction and Filtering Techniques. *International Journal of Science and Research (IJSR)*, Vol. 6, No. 3, pp.2033–2038. https://doi.org/ 10.21275/25031706.
18. Heo, Y., Kyuseok, K. and Youngjin, L. (2020). Image Denoising Using Non-Local Means (NLM) Approach in Magnetic Resonance (MR) Imaging: A Systematic Review. *Applied Sciences*, Vol. 10, No. 20, pp.7028-7028. https://doi.org/10.3390/app10207028.
19. Hore, A. and Djemel, Z. (2010). Image Quality Metrics: PSNR vs. SSIM. *2010 20th International Conference on Pattern Recognition*. No. 22. https://doi.org/10.1109/icpr.2010.579.
20. Huihua, K., Gao, W. and Di, Y. (2023). An Improved Non-Local Means Algorithm for CT Image Denoising, No. 25. https://doi.org/10.21203/rs.3.rs-2915903/v1.
21. Hussein, Mohammad M. Faqe. "Comparison of Time Series Models before and after Using Wavelet Shrinkage Filtering to Forecast the Amount of Natural Gas in Iraq." *Cihan University-Erbil Scientific Journal (CUESJ)* 6, no. 1 (2022): 32–46.
22. Kaur, B., Ayush, D. and Bhawna G. (2020). Comparative Analysis of Bilateral Filter and Its Variants for Magnetic Resonance Imaging. *The Open Neuroimaging Journal*, Vol. 13, No. 1, pp.21–29. https://doi.org/10.2174/1874440002013010021.
23. Kolhe, Y. and Yogendra, J. (2013). Removal of Salt and Pepper Noise from Satellite Images. *International Journal of Engineering Research and Technology (IJERT)*, Vol. 2, No. 11, pp.2051–2058. https://doi.org/10.17577/IJERTV2IS110634.
24. Liu, B. and Jianbin, L. (2018). Non-Local Mean Filtering Algorithm Based on Deep Learning. *MATEC Web of Conferences*, Vol. 23, No. 2. https://doi.org/10.1051/matecconf/201823203025.
25. Liu, W., Pingping, Z., Xiaogang, C., Chunhua, S., Xiaolin, H. and Jie, Y. (2020). Embedding Bilateral Filter in Least Squares for Efficient Edge-Preserving Image Smoothing. *IEEE Transactions on Circuits and Systems for Video Technology*, Vol. 30, No. 1, pp.23–35. https://doi.org/10.1109/tcsvt.2018.2890202.
26. Muslim, A. and Ghalib, A. (2019). Comparison Between the Method of Principal Component Analysis and Principal Component Analysis Kernel for Imaging Dimensionality Reduction. *Journal Of Economics and Administrative Sciences*, Vol. 16, No. 2, pp.11–24. https://doi.org/https://doi.org/10.33899/iqjoss.2019.164189.
27. Muslim, A. and Ghalib, A. (2019). Use Principal Component Analysis Technique to Dimensionality Reduction to Multi-Source. *Journal Of Economics and Administrative Sciences*, Vol. 25, No. 115, pp.464–473. https://doi.org/https://doi.org/10.33095/jeas.v25i115.1778.
28. Nabahat, M., Farzin, K. and Nima, N. (2022). Optimization of Bilateral Filter Parameters Using a Whale Optimization Algorithm. *Research in Mathematics*, Vol. 9, No. 1. https://doi.org/10.1080/27684830.2022.2140863.
29. Sarker, S. (2012). Use of Non-Local Means Filter to Denoise Image Corrupted by Salt and Pepper Noise. *Signal and amp Image Processing: An International Journal*, Vol. 3, No. 2, pp.223–235. https://doi.org/10.5121/sipij.2012.3217.
30. Swamy, S. and Kulkarn, P. (2020). A BASIC OVERVIEW OF IMAGE DENOISING TECHNIQUES. *International Research Journal of Engineering and Technology (IRJET)*, Vol. 7, No. 5, pp.850–857.
31. Tomasi, C. and Manduchi, R. (2005). Bilateral Filtering for Gray and Color Images. *Sixth International Conference on Computer Vision (IEEE Cat. No.98CH36271)*. Vol 22, No. 16. https://doi.org/10.1109/iccv.1998.710815.
32. Wagner, F., Mareike, T., Felix, D., Mingxuan, G., Mayank, P., Stefan, P., Noah, M., Laura, P., Yixing, H. and Andreas, M. (2022). Trainable Joint Bilateral Filters for Enhanced Prediction Stability in Low-Dose CT. *Scientific Reports*, Vol. 12, No. 1. https://doi.org/10.1038/s41598-022-22530-4.
33. Wagner, F., Mareike, T., Mingxuan, G., Yixing, H., Sabrina, P., Mayank, P. and Stefan, P. (2022). Ultralow-parameter Denoising: Trainable Bilateral Filter Layers in Computed Tomography. *Medical Physics*, Vol. 49, No. 8, pp.5107–5120. https://doi.org/10.1002/mp.15718.
34. Wang, Z., Bovik, C. Sheikh, R. and Simoncelli, P. (2004). Image Quality Assessment: From Error Visibility to Structural Similarity. *IEEE Transactions on Image Processing*, vol. 13, No. 4, pp.600–612. https://doi.org/10.1109/tip.2003.819861.
35. Wilson, B. and Julia, D. (2013). A Survey of Non-Local Means Based Filters for Image Denoising. *International Journal of Engineering Research and Technology (IJERT)*, Vol. 2, No. 10, pp.3768–3771.
36. You, J. and Nam, C. (2013). An Adaptive Bandwidth Nonlocal Means Image Denoising in Wavelet Domain. *EURASIP Journal on Image and Video Processing*, No. 1. https://doi.org/10.1186/1687-5281-2013-60.